Sensitive Fluorescence Polarization Technique for Rapid Screening of α-Synuclein Oligomerization/Fibrillization Inhibitors

Kelvin C. Luk, Edward G. Hyde, John Q. Trojanowski, and Virginia M.-Y. Lee*

Center for Neurodegenerative Disease Research, Department of Pathology and Laboratory Medicine, University of Pennsylvania, Philadelphia, Pennsylvania 19143

Received June 7, 2007; Revised Manuscript Received August 20, 2007

ABSTRACT: Parkinson's disease (PD) is characterized by the accumulation of fibrillar α-synuclein (α-Syn) inclusions known as Lewy bodies (LBs) and Lewy neurites. Mutations in the α-Syn gene or extra copies thereof cause familial PD or dementia with LBs (DLB) in rare kindreds, but abnormal accumulations of wildtype α-Syn also are implicated in the pathogenesis of sporadic PD, the most common movement disorder. Insights into mechanisms underlying α-Syn mediated neurodegeneration link α-Syn oligomerization and fibrillization to the onset and progression of PD. Thus, inhibiting α-Syn oligomer or fibril formation is a compelling target for discovering disease modifying therapies for PD, DLB, and related synucleinopathies. Although amyloid dyes recognize α-Syn fibrils, efficient detection of soluble oligomers remains a challenge. Here, we report a novel fluorescence polarization (FP) technique for examining α-Syn assembly by monitoring changes in its relative molecular mass during progression of normal α-Syn from highly soluble monomers to higher order multimers and thence insoluble amyloid fibrils. We report that FP is more sensitive than conventional amyloid dye methods for the quantification of mature fibrils, and that FP is capable of detecting oligomeric α-Syn, allowing for rapid automated screening of potential inhibitors of α-Syn oligomerization and fibrillization. Furthermore, FP can be combined with an amyloid dye in a single assay that simultaneously provides two independent biophysical readouts for monitoring α-Syn fibrillization. Thus, this FP method holds potential to accelerate discovery of disease modifying therapies for LB PD, DLB, and related neurodegenerative synucleinopathies.

Aggregates of misfolded proteins are features of aging-related neurodegenerative disorders, and deposits of misfolded disease-specific proteins form signature lesions of Alzheimer's disease (AD), Parkinson's disease (PD), and related conditions. For example, the neuropathological hallmarks of PD, the most common neurodegenerative movement disorder, are neuronal inclusions known as Lewy bodies (LBs) and Lewy neurites (LNs) formed by accumulations of α-synuclein (α-Syn) fibrils (*1*, *2*). The precise function of α-Syn is unknown, as are the mechanisms by which it mediates the dysfunction and degeneration of neurons. LBs and LNs also define an AD-like cognitive disorder known as dementia with LBs (DLB) while α-Syn fibrils accumulate in glial cells to form the signature inclusions of multiple system atrophy, a rare PD-like movement disorder (*3*, *4*). Hence, these and other neurodegenerative disorders characterized by fibrillar α-Syn amyloid lesions are known as synucleinopathies (*5*).

Multiple lines of evidence implicate misfolding, oligomerization, and fibrillization of α-Syn in mechanisms of neurodegeneration in PD, DLB, and related synucleinopathies (*6*−*10*), a revolution in mechanistic understanding which was initiated by the identification of mutations in the gene encoding α-Syn as well as by the demonstration that α-Syn is the principal component of filamentous LBs and LNs (*11*−*13*). Indeed, these and subsequent insights into the normal biology of α-Syn and the role of α-Syn pathologies in neurodegeneration are reorienting the design of drug discovery efforts for PD and related synucleinopathies to focus on targets related to α-Syn misfolding, oligomerization, and fibrillization (*5*).

Understanding α-Syn fibril assembly is increasingly critical for the discovery of disease modifying therapies for PD and related synucleinopathies, but integral to these efforts is the availability of sensitive, reliable, and accessible methods for distinguishing soluble (monomeric and oligomeric) and insoluble (amyloid and non-amyloid) forms of α-Syn. This is particularly challenging because α-Syn is a heat-stable, natively unfolded protein with no well-defined activity for monitoring changes in the biophysical state of normal α-Syn as it converts to pathological soluble oligomers and insoluble fibrils (*14*, *15*). Currently established screening methods for anti-fibril agents utilize traditional amyloid binding dyes such as Thioflavin T (ThT), Congo Red, and derivatives thereof such as K114 (*16*), but all these share the limitation of having variable and ill-defined amyloid binding sites (*17*, *18*). Furthermore, they are susceptible to optical and fluorescence interference, and they fail to detect pre-fibrillar intermediates. Although other methods such as electron microscopy (EM), filter traps, and sedimentation analysis have relevant applications for monitoring amyloidogenesis (*19*), they are not amenable to high-throughput screening (HTS) strategies.

* To whom correspondence should be addressed. Tel.: 215-662-6427. Fax: 215-349-5909. E-mail: vmylee@mail.med.upenn.edu.

10.1021/bi701128c CCC: $37.00
Published on Web 10/10/2007

Increasingly, attention has focused on non-fibrillar oligomeric α-Syn as a possible source of toxicity in PD (*20*, *21*). Oligomeric intermediates have been described using spectroscopic techniques, immunological detection, size exclusion chromatography, and atomic force microscopy (*9*, *10*, *14*, *22*−*24*). However, these methods are arduous, difficult to quantify, and often require specialized equipment. The application of fluorescence correlation spectroscopy for examining α-Syn assembly in vitro has been reported (*25*), but it remains uncertain if this method detects smaller intermediates. Thus, there is an urgent need for more effective and scalable methods for rapidly monitoring α-Syn oligomerization and fibrillization.

As free rotation of fluorescent moieties in solution is inversely proportional to relative molecular mass, processes that affect the movement of a fluorescently tagged object, e.g., association into larger complexes, can be effectively monitored using fluorescence polarization (FP) technology (*26*). Hence, we hypothesized that free rotation of fluorophore-linked α-Syn would be hindered during the course of assembly as monomers associate to form larger intermediates and ultimately insoluble fibrils. We report here that changes in FP of labeled α-Syn during assembly can be effectively monitored by this method. Moreover, FP is not only more sensitive than the amyloid dyes tested here for the detection of mature fibrils, but it also recognizes soluble α-Syn oligomers in addition to α-Syn fibrils. Therefore, this method represents a novel tool for drug discovery focused on inhibiting α-Syn polymerization.

EXPERIMENTAL PROCEDURES

Protein Purification. Recombinant wild type (WT) human α-Syn was expressed in *Escherichia coli* BL21-RIL (Stratagene, La Jolla, CA) and purified as previously described (*27*) with minor modifications. Briefly, clarified lysate was separated by gel filtration following precipitation of heat-sensitive proteins by boiling. Fractions containing α-Syn were then pooled and eluted over a 0.1−1.0 M NaCl gradient from a HiTrap Q column (GE Healthcare, Piscataway, NJ) equilibrated with Tris (50 mM, pH 7.5). Protein purity was assessed by Coomassie blue staining. Proteins were dialyzed into 50 mM Tris (pH 7.0, containing 100 mM NaCl), concentrated, and stored at −80 °C in aliquots until used. Protein concentrations were measured using a BCA protein quantification kit (Pierce, Rockford, IL) with bovine serum albumin as a standard.

Fluorescent Labeling of α-Syn. Labeling with Oregon Green 488 or Alexa Fluor 594 was achieved by reacting succinimidyl-ester forms of the dyes with purified α-Syn. Following dialysis against phosphate buffered saline (PBS), α-Syn was labeled with the Oregon Green 488 or Alexa Fluor Red 594 labeling kits (Molecular Probes, Eugene, OR) according to the manufacturer's instructions. The concentration of α-Syn was titrated to achieve a labeling molar ratio of ∼1:10 (dye to protein). Unbound dye was removed by extensive dialysis into 50 mM Tris (pH 7.0).

Fibril Assembly Reactions. Purified α-Syn was passed through a 0.22 μm cellulose acetate filter to remove any aggregates and was then diluted to a final concentration of 1 mg/mL (∼72 μM) in assembly buffer (50 mM Tris, 100 mM NaCl, pH 7.0). Fibril assembly was performed either in low-volume 384-well polycarbonate plates (Nunc, Rochester, NY) (20 μL per reaction) or in 200 μL microcentrifuge tubes (100 μL per reaction) at 37 °C in an orbital mixer providing constant agitation at 1000 rpm.

For experiments designed to test inhibitors of fibrillization/oligomerization, reactions containing 2 mg/mL α-Syn were performed in potassium acetate buffer (50 mM, pH 7.0) containing 50 mM KCl and 5 mM $MgCl_2$. Dopamine hydrochloride, dihydroxy-l-phenylalanine (L-DOPA), epinephrine, norepinephrine, and baicalein were obtained from Sigma (St Louis, MO) and dissolved in DMSO just prior to addition to assembly reactions. Inhibitors were used at a final concentration of 50−200 μM. Accompanying reactions containing an identical concentration of DMSO (2%) were included as controls.

ThT and K114 Assays. At various time points, 10 μL aliquots were removed from reactions and mixed with 100 μL of glycine (100 mM, pH 8.5) containing 20 μM Thioflavin T (ThT; Sigma), an amyloid specific binding dye. Fluorescence intensity was read at 470 nm/510 nm (ex/em; cutoff 495 nm) using a Spectramax M5 plate reader (Molecular Devices, Sunnyvale, CA). Parallel aliquots from the same reactions were also added to 100 μM (*trans,trans*)-1-bromo-2,5-bis-(4-hydroxy)styrylbenzene (K114), a highly sensitive amyloid binding dye (*15*), in 100 mM glycine (pH 8.5), and fluorimetry was performed at 380 nm/550 nm (530 nm cutoff) as previously described (*16*).

Fluorescence Polarization. For FP experiments, fibril assembly reactions were performed as described above with labeled α-Syn added at a final dye to protein ratio of 1:250 to 1:100. Unlabeled α-Syn was adjusted to maintain a constant concentration of 1 mg/mL total α-Syn. Fluorescence in both perpendicular and parallel planes was recorded at various time points during reactions using a Spectramax M5 reader (average of 100 measurements/sample). Oregon Green and Alexa Fluor 594 labeled α-Syn were detected at 490/525 nm and 590/620 nm, respectively. After subtraction of background fluorescence, FP values were calculated and expressed as change in milli-polarization units (ΔmP) relative to free labeled monomer.

Sedimentation and Immunoblot Analyses. Reactions were subjected to ultracentrifugation (100 000*g*) for 30 min over a sucrose cushion at 4 °C. Both the pellet and supernatant were recovered and separately measured for Oregon Green or Alexa Fluor Red fluorescence. Samples were then re-suspended in SDS sample buffer, boiled for 10 min, and separated by SDS-PAGE (15%). Proteins were revealed by staining with Coomassie blue.

Negative-Stain EM and Immuno-EM. For EM, assembly reactions were adsorbed onto 300-mesh carbon-coated copper grids and negatively stained with 1% uranyl acetate. For immuno-EM, grids were incubated with primary antibodies against α-Syn (SNL-1, 1:100) or Oregon Green 488 (monoclonal anti-fluorescein; Molecular Probes, 1:200). Grids were visualized after incubation with colloidal gold-conjugated (10 or 16 nm) secondary antibodies against rabbit or mouse immunoglobulins, respectively (1:20) (Aurion, Wageningen, The Netherlands), and negative staining on a JEOL 1010 transmission electron microscope. Images were captured with a digital camera (Hamamatsu, Bridgewater, NJ) using AMT acquisition software.

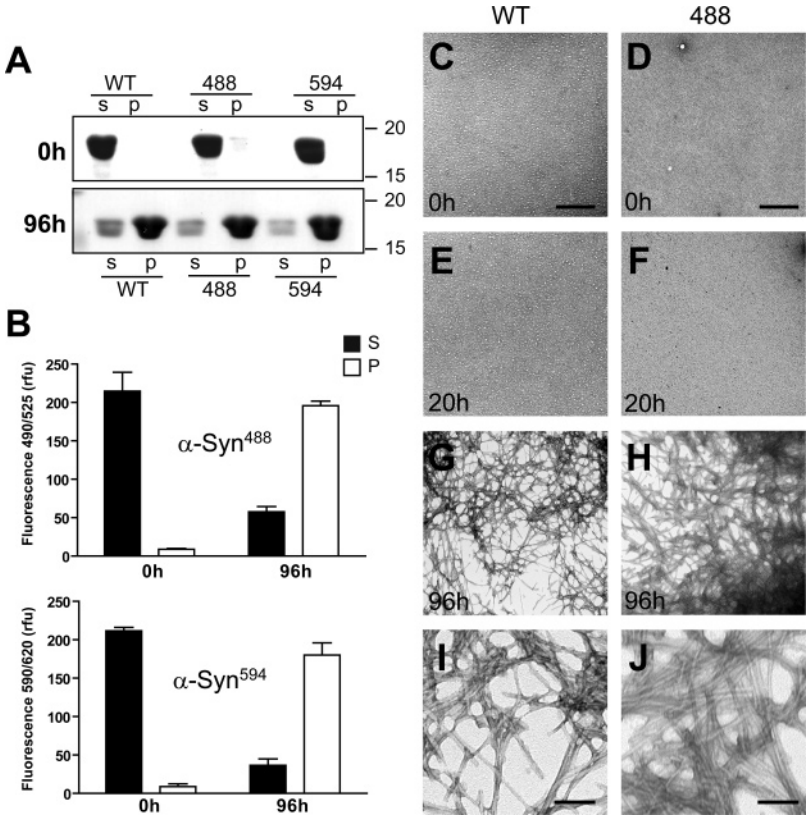

FIGURE 1: Aggregation of fluorescently labeled α-Syn. (A) Assembly reactions containing only WT α-Syn or WT α-Syn spiked with either α-Syn^{488} or α-Syn^{594} (1:200 final dye to protein ratio) were performed in low volume 384-well plates. At 0 or 96 h after incubation and agitation, products were separated by SDS electrophoresis (15%) following centrifugation. Distribution of protein between the supernatant (s) and pellet (p) fraction was comparable for all three conditions at the time points examined. (B) Fluorescence intensity of supernatant (s) and pellet (p) fractions in reactions containing α-Syn^{488} or α-Syn^{594}, showing that labeled α-Syn partitions in a manner similar to unlabeled α-Syn in both unassembled (0 h) and completed (96 h) reactions (data represents mean ± SD, $n = 3$). (C−J) Negatively stained EM views of assembly reactions containing WT α-Syn or α-Syn^{488} at various time points. Fibrils with similar morphology were observed in reactions containing α-Syn^{594} (data not shown). Scale bars: C−H, 500 nm; I and J, 100 nm.

RESULTS

Fluorescent Labeling of α*-Syn.* In order to facilitate real-time, nondestructive detection of α-Syn in vitro, we independently labeled purified recombinant α-Syn using either of two fluorescent dyes with distinguishable spectral properties. Incubation of the reactive succinimidyl esters of either Oregon Green 488 or Alexa Fluor 594 respectively yielded α-Syn^{488} and α-Syn^{594}. In addition to their photostability relative to traditional dyes such as fluorescein, both fluorophores exhibit minimal fluctuation at neutral pH values (*28*). To minimize possible interference with fibril assembly, labeling was performed to ensure that the final dye:protein molar ratio did not exceed one. Despite the small quantities of attached fluorophore, labeled α-Syn could be readily detected by spectrophotometry at sub-micromolar concentrations, providing sufficient sensitivity for subsequent assays.

Fluorescent Tagged α*-Syn Assembles into Fibrils.* We determined whether fluorescently conjugated α-Syn species share similar in vitro aggregation properties with unlabeled WT α-Syn by comparing reactions initially containing monomeric WT α-Syn with those spiked with small quantities of α-Syn^{488} or α-Syn^{594}. In reactions containing only WT α-Syn, the majority of α-Syn could be sedimented within 96 h of incubation and agitation, reflecting the formation of aggregates (Figure 1A). Likewise, α-Syn predominantly partitioned into the insoluble fraction after 96 h in reactions containing either α-Syn^{488} or α-Syn^{594} (Figure 1A). In agreement with this finding, the bulk of detectable fluorescence intensity shifted from the soluble fraction at 0 h to the insoluble fraction at 96 h by the same extent in both α-Syn^{488} or α-Syn^{594} reactions (Figure 1B). Changes in total fluorescence intensity were minimal, in agreement with previous studies (*25*), suggesting minimal photobleaching and that the labeled residues are not sequestered within the hydrophobic fibril core (*29*).

To determine whether aggregates containing α-Syn^{488} and α-Syn^{594} resembled typical amyloid fibrils formed by WT α-Syn alone, reaction products from assemblies performed in 384-well plates were examined by EM at multiple time points (Figure 1C−J). At incubation times of 0 and 20 h, neither unlabeled nor fluorescent α-Syn assembled into structures discernible by EM. However, after 96 h incubation, negative staining EM revealed abundant rod-like structures (10−14 nm diameter) typical of amyloid fibrils that were indistinguishable between unlabeled and α-Syn^{488}-containing samples (Figure 2G−J). Similar fibrils were also observed in reactions containing α-Syn^{594} (data not shown). Collectively, these findings demonstrate that the covalent addition of a small fluorescent tag does not interfere with efficient α-Syn fibrillization. Moreover, the similar time course for appearance of fibrils in reactions containing α-Syn^{488} (Figure 1D,F,H) or unlabeled α-Syn alone (Figure 1C,E,G) indicate that they share comparable assembly kinetics and fibril morphology.

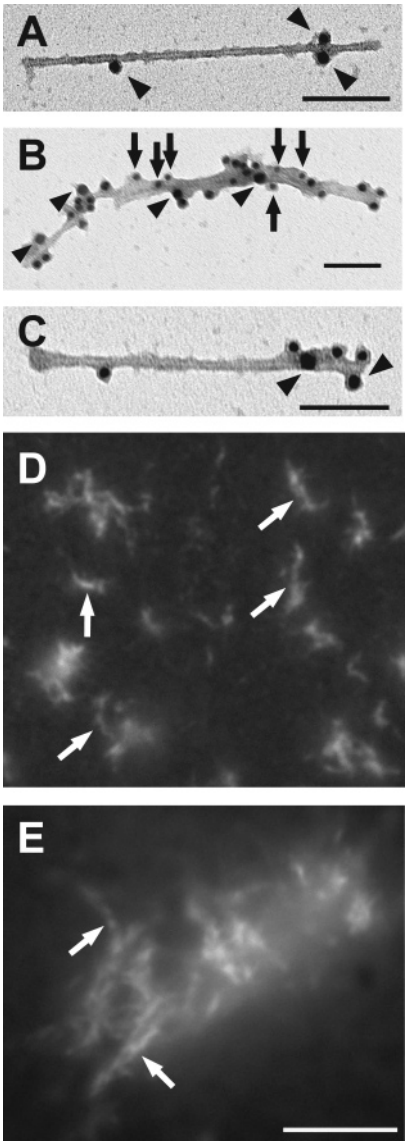

FIGURE 2: α-Syn^{488} and α-Syn^{594} are incorporated into fibrils. Immuno-EM images of fibrils from samples containing α-Syn^{488} after 96 h: (A) single immunogold labeling of Oregon Green 488 using an antibody against fluorescein (arrowheads) indicating the presence of fluorescent dye on individual synuclein fibrils; (B, C) double immunogold labeling of Oregon Green 488 (arrowheads) and α-Syn with SNL-1 antibody (arrows) (*30*) on individual fibrils. Material from reactions containing WT α-Syn with either α-Syn^{488} (D) or α-Syn^{594} (E) visualized using conventional fluorescence microscopy using appropriate filters revealed aggregated fibrillar structures. Scale bars = 100 nm for A−C; 5 μm for D and E.

Labeled α-Syn Is Incorporated into Fibrils. We examined whether labeled α-Syn molecules were incorporated into the fibrils observed by EM. Immunostaining using specific antibodies recognizing α-Syn (SNL-1) (*30*) or Oregon Green 488 (anti-fluorescein) revealed immunogold particles along the axis of individual fibrils in 96 h samples containing α-Syn^{488}, demonstrating that α-Syn^{488} was incorporated into filaments (Figure 2A). Double immuno-EM for Oregon Green (arrowheads, large gold particles) and α-Syn (arrows, small gold particles) confirmed these as α-Syn fibrils (Figure 2B,C). Abundant fibrillar structures could also be visualized in reactions containing α-Syn^{488} or α-Syn^{594} by conventional fluorescence microscopy at high magnification (Figure 2D,E), even though the concentration of labeled α-Syn represents less than 1% of that required for fibril formation under these conditions. Taken together, these data demonstrate that WT and labeled α-Syn readily co-assemble into amyloid fibrils comparable to those formed by the unmodified wildtype protein alone.

Monitoring Fibril Assembly Using FP. Changes in the free rotation of fluorescent moieties in solution can be readily detected using FP. Rapid rotation correlates with a reduction in polarization, whereas decreased rotation results in higher polarization. In turn, rotation is inversely proportional to relative molecular mass, so that processes which affect the movement of a fluorescently tagged object, e.g., assembly into larger intermediates, can be effectively monitored using FP (*26*, *31*). Consistent with our initial hypothesis, FP values of reactions containing either α-Syn^{488} or α-Syn^{594} increased during the course of assembly suggesting a substantial increase in the molecular size of the complex containing the fluorescent protein (Figure 3A). Polarization values in α-Syn^{488} reactions closely matched those of α-Syn^{594} reactions throughout the entire timecourse, indicating that both labeled proteins behaved in a similar fashion.

To further investigate whether this change in FP correlated with the progression of monomer to various multimeric species, we concommitantly monitored amyloid fibril assembly during this period in both α-Syn^{488} and α-Syn^{594} reactions using ThT and K114, two well-established amyloid binding dyes with distinct binding properties (*16*, *18*, *32*). Since ThT and Alexa Fluor overlap minimally in their fluorescence spectra, we were able to directly simultaneously collect both FP and ThT data from samples. To ensure labeled α-Syn did not interfere with readings from amyloid dyes in α-Syn^{488} reactions, ThT and K114 fluorescence were measured in parallel samples. As expected, both ThT and K114 measurements exhibited similar exponential rises in fluorescence intensity preceded by a lag phase of 30−40 h (Figure 3B,C) and consistent with a nucleation-dependent process described for assembly (*7*). Interestingly, increases in FP were observable within approximately 20 h after initiation of the reaction in both α-Syn^{488} and α-Syn^{594} reactions—significantly earlier than the end of the lag phase as detected by either amyloid dye, suggesting that FP may be detecting an intermediate or pre-fibrillar species of α-Syn that is not recognized by amyloid dyes like ThT and K114. Alternatively, FP may recognize fibrils with more sensitivity than either ThT or K114.

To resolve this issue, we used EM to examine the α-Syn species at different times of incubation. Significantly, numerous spherical species could be observed at 30 h corresponding to an intermediate FP value but not at 0 h (Figure 3D,E). In contrast, fibrils were profuse at 72 h at which time FP values had reached a plateau (Figure 3F), suggesting that oligomers are sensitive to detection by FP. Together with the observation that maximal FP values (∼150 mP units above monomer) were attained approximately 50 h after initiation before saturation of ThT fluorescence, this likely reflects the upper detection limit for this method. However, since our method provides the collective FP value for each sample rather than of individual α-Syn^{488}-containing complexes, the relative contributions by monomer, oligomer, and fibrils to the observed FP should be considered. In addition, although increases in FP correlate with molecular mass, the relationship may not be a linear one owing to the nonparametric nature of the measurements.

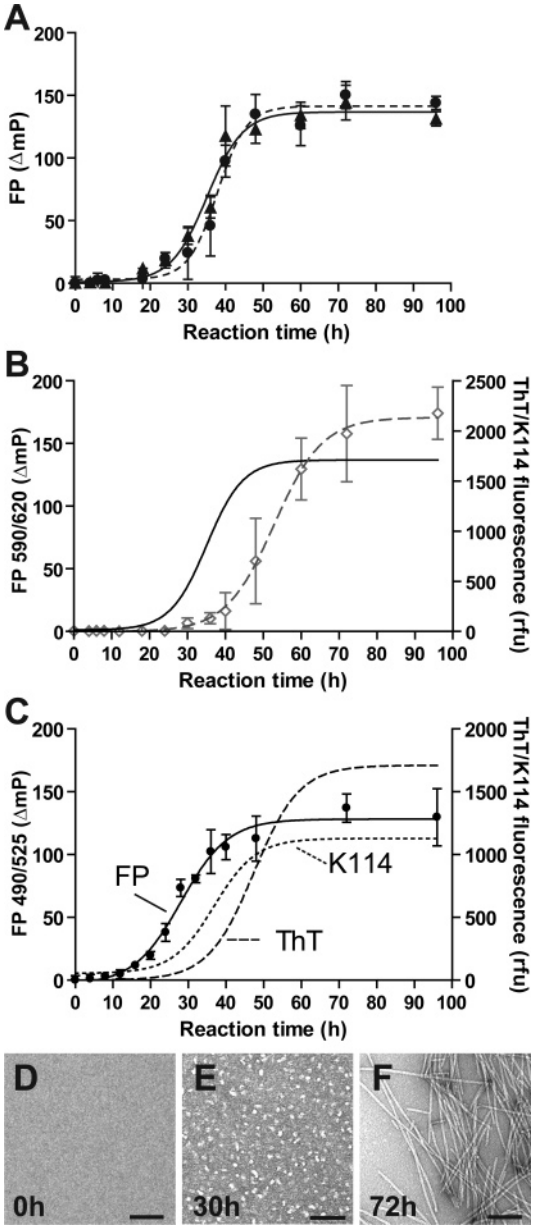

FIGURE 3: Fluorescence polarization of labeled α-Syn. Changes in the rotational state of α-Syn^{488} or α-Syn^{594} were measured by FP as described in Experimental Procedures. Reactions were performed in 384-well plates, and individual samples were removed and measured at the indicated time points. (A) Changes in FP relative to monomer (ΔmP) in reactions containing α-Syn^{488} (circles) or α-Syn^{594} (triangles) over a 96 h incubation period indicating that FP increases significantly following assembly. Data (means ± SD, $n = 3$) were fitted to a variable slope sigmoidal curve using GraphPad Prism software. (B) Individual assembly reactions containing α-Syn^{594} from part A were also measured for ThT fluorescence (diamonds, dashed line) over the course of assembly. FP from the same samples (solid line) is also shown. (C) Unlabeled and α-Syn^{488} assembly reactions were performed in parallel. ThT and K114 fluorescence was measured in unlabeled samples and compared to FP values from α-Syn^{488} reactions at each time point. Data are expressed as mean ± SEM from at least two experiments ($n = 3$). Negatively stained EM of α-Syn^{488} reactions at 0 (D), 30 (E), and 72 h (F) are shown, corresponding to the baseline, intermediate, and maximal FP values in part C.

FP Detection of α-Syn Oligomers and Fibrils. To further establish that the observed increase in FP is due to the formation of α-Syn/α-Syn^{488} oligomers, we compared the FP values of different α-Syn species separated by size exclusion chromatography, a technique that effectively isolates α-Syn monomers, dimers, and soluble oligomers (*20*, *24*, *33*). After a short centrifugation step to eliminate α-Syn fibrils, the soluble fraction was loaded onto the column and Oregon Green fluorescence intensity was used to monitor α-Syn^{488} in fractions eluted from the soluble phase of reactions at 0, 6, 16, and 30 h (Figure 4A). While a single population, representing monomer, was detected following separation of 0 h α-Syn^{488} reactions, multiple species with reduced elution times were detectable at subsequent time points (6, 16, and 30 h), indicating the presence of both monomeric and oligomeric α-Syn^{488} as reactions progressed. Interestingly, the main oligomeric peak in these reactions eluted slightly earlier than α-Syn^{488} preparations containing dopamine, which generates stable soluble oligomers, indicating that the former may represent a larger soluble species.

FP analysis of individual fractions revealed a clear correlation between molecular radius (elution time) and increase in FP (Figure 4B). In contrast to monomeric species which exhibited baseline values at all reaction times examined, FP values increased with mass in other fractions containing α-Syn^{488}. Maximal FP values from soluble samples (~135 mP) were observed in species eluting close to the void volume, indicating that this assay can readily distinguish α-Syn oligomers from monomers. Fractions containing dopamine stabilized oligomers exhibited slightly lower FP values, in agreement with their order of elution from the size exclusion column.

To confirm these fractions contained distinct forms of α-Syn, fractions representative of monomers and higher molecular-weight species were examined by negative-stain EM (Figure 4C−F). We observed numerous spherical oligomeric structures in representative fractions of oligomers (eluting at 16−18 min) by EM following negative staining (Figure 4C). Maximum diameters ranged from 15 to 35 nm for these structures, comparable to that of spontaneously occurring α-Syn oligomers as well as oligomers stabilized by catecholamines (*20*, *34*). In contrast, we could not distinguish objects in later fractions (eluting at 30−32 min) consistent with a preponderance of monomeric content (Figure 4D). Comparable results were obtained from fractions separated from reactions containing either α-Syn^{488}, α-Syn^{594}, or unlabeled α-Syn alone (Figure 4C,E and data not shown). The observation that soluble oligomeric species with nearly identical morphological features and molecular mass could be recapitulated with labeled α-Syn further supports our earlier observation that the fluorescently tagged and untagged α-Syn behave similarly.

Monitoring α-Syn Assembly Inhibition Using FP. To further ascertain its ability to distinguish between monomeric and oligomeric forms of α-Syn, we then used FP to monitor the state of labeled α-Syn in the presence of known inhibitors of fibril formation. Although α-Syn^{488} and α-Syn^{594} display similar assembly characteristics under the conditions described here, we selected α-Syn^{594} in order to minimize fluorescence interference arising in the green portion of the spectrum that is typical of many compounds used in HTS libraries. Additionally, we were able to exploit the absorbance/emission range of α-Syn^{594}, which allowed simultaneous detection of amyloid fibrils by using ThT within individual samples.

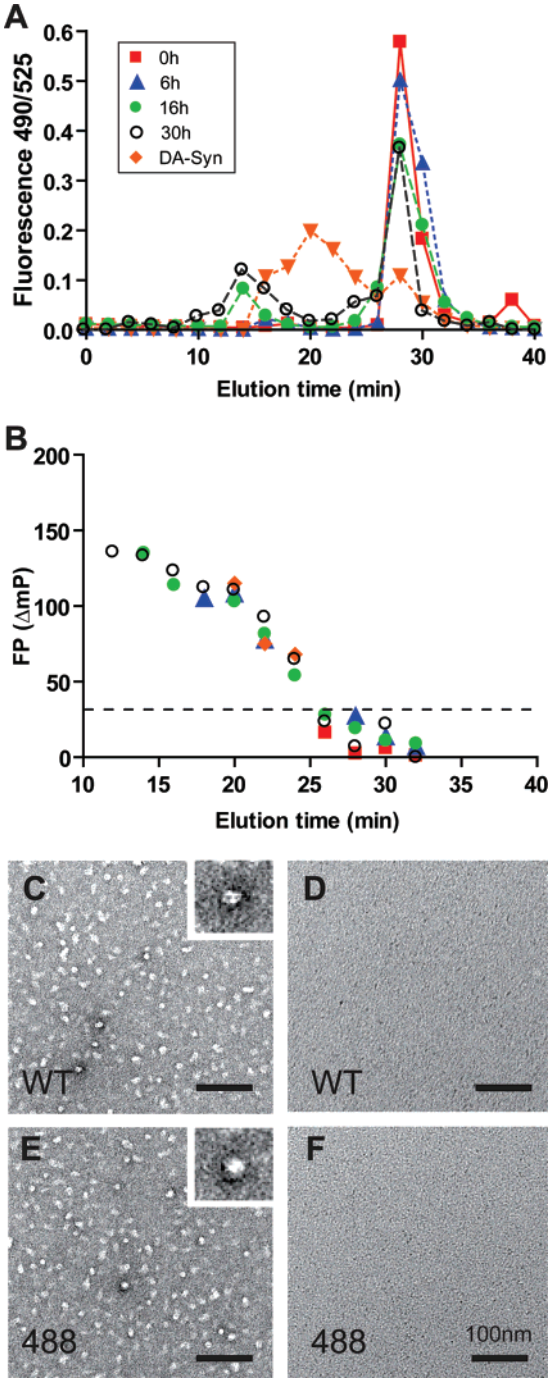

FIGURE 4: Correlation between FP and mass of α-Syn species. (A) Samples containing 2 mg/mL α-Syn were spiked with α-Syn^{488} (1:200) and incubated for 0, 4, 16, or 30 h (represented by squares, triangles, filled circles, and open circles, respectively). At each time point, 100 μL of sample was spun briefly to remove fibrils and loaded onto a Superdex 200 column. Oregon Green 488 fluorescence intensity was quantified for each eluted fraction. The separation profile of the α-Syn^{488} reaction following 48 h treatment with dopamine (DA-Syn) is also shown (diamonds). (B) Individual fractions containing α-Syn^{488} were measured for FP and plotted as a function of elution time. FP values of monomeric fractions were within a narrow range (dotted line), whereas increasing the molecular size of α-Syn^{488} containing complexes correlated with higher FP values. (C−F) Electron micrographs of monomer or oligomer fractions negatively stained with 1% uranyl acetate at 16 h. (C, E) Early eluting fractions (~16 min) from samples containing unlabeled α-Syn or α-Syn^{488} exhibited numerous objects 15−30 nm in diameter consistent with oligomers (inset). (D, F) Fractions corresponding to monomeric α-Syn did not contain discernible structures under these conditions.

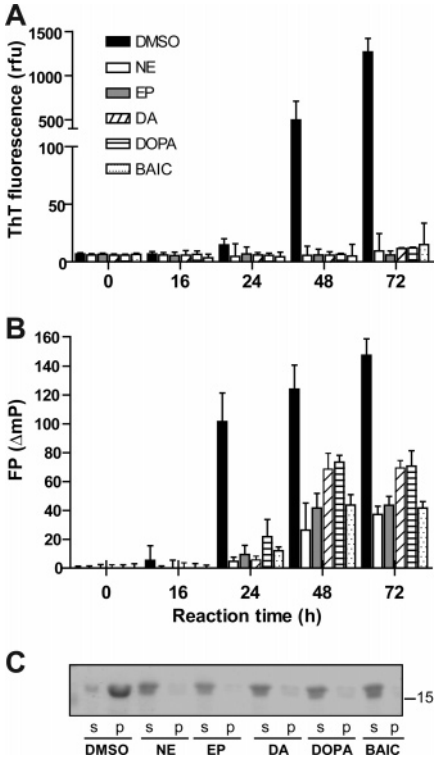

FIGURE 5: FP detection of α-Syn fibril assembly inhibition. Reactions containing α-Syn^{594} (100 μL) were incubated in the presence of inhibitors of fibrillization or DMSO for up to 48 h in microfuge tubes. Total α-Syn concentration was adjusted to 2 mg/mL. At various time points, inhibition was quantified in individual samples treated with norepinephrine (NE; 200 μM), epinephrine (EP; 100 μM), dopamine (DA; 100 μM), L-DOPA (DOPA; 50 μM), or baicalein (100 μM) by ThT fluorescence (A). (B) Fluorescence polarization measurements of the same reactions following incubation with compounds showing stabilization of multimeric intermediates by inhibitors. Results are expressed as the mean change in FP ± SEM from two independent experiments ($n = 3$). Inhibition of fibril formation was confirmed by electrophoresis and Coomassie staining of soluble (s) and pelletable (p) material from each sample (C).

Assembly reactions containing α-Syn (2 mg/mL) spiked with α-Syn^{594} were separately incubated in the presence of compounds previously reported to inhibit α-Syn fibrils through distinct mechanisms (Figure 5). Both catecholamines (*20*, *35*) and the flavinoid baicalein (*36*) have been shown to stabilize soluble oligomeric forms of α-Syn while preventing the accumulation of fibrillar species. In the presence of vehicle (DMSO) alone, assembly of α-Syn^{594} produced aggregates with β-rich sheet structure as indicated by increased ThT fluorescence and turbidity. As expected, addition of norepinephrine (200 μM), epinephrine (100 μM), dopamine (100 μM), or L-DOPA (50 μM) resulted in a reduction of ThT fluorescence by over 98% after 72 h (Figure 5A). Similarly, the presence of 100 μM baicalein also prevented amyloid formation by 97% as measured by ThT fluorescence.

When the inhibition of α-Syn fibril formation was examined using FP, initial FP values were comparable in the presence of all five compounds, indicating the lack of any significant interference with the fluorescent label (Figure 5B). In contrast to DMSO control reactions in which ΔmP values exceeded 100 by 24 h, samples containing baicalein or catecholamines displayed only minor increases (<40 mP),

consistent with their ability to inhibit aggregation. However, an intermediate increase in FP was observable by 48 h and remained constant at 72 h, suggesting the presence of non-monomeric species containing α-Syn^{594}. Consistent with ThT and FP results, the majority of α-Syn remained soluble in the presence of all compounds while the proportion of pelletable protein increased significantly in reactions containing only DMSO (Figure 5C). Given that sedimentation analysis and ThT precluded any significant quantity of insoluble fibrils in the soluble fractions, and since previous studies have demonstrated inhibition of α-Syn elongation and not nucleation, the FP detected here likely reflects the presence of soluble oligomers containing α-Syn^{594} formed by modification with inhibitory compounds. Furthermore, the measured FP values fall within the range observed earlier for α-Syn oligomers (Figure 4B). Thus, FP faithfully reports the state of labeled α-Syn in the presence of compounds that modulate fibrillization, including those which favor non-fibrillar intermediates as end products.

DISCUSSION

We describe here a novel FP-based method that detects oligomeric and fibrillar species of α-Syn. Hence, FP can be used to monitor the dynamic process of α-Syn fibrillization, a central event in the pathogenesis of PD, and an increasingly compelling target for the discovery of disease modifying therapies to treat PD and related synucleinopathies. Indeed, based on literature summarized above and reviewed elsewhere (*5*), there are multiple reasons to target pathological species of α-Syn to develop more effective interventions for these disorders. Thus, the novel screening methods described here are likely to accelerate the pace of these efforts.

The FP method we developed depended on the detection of α-Syn by attaching photostable fluorophores to α-Syn. Notably, we demonstrate that labeled α-Syn and its unlabeled counterpart share similar aggregation properties for the following reasons: (1) Aggregation of labeled α-Syn exhibits the same assembly kinetics as unlabeled α-Syn, characterized by an extensive lag phase presumably reflecting nucleation. (2) Labeled α-Syn co-assembles with unlabeled α-Syn into fibrils with identical morphology as those formed by unmodified α-Syn alone. (3) No preferential incorporation of either labeled or unlabeled α-Syn into fibrils occurred as labeled α-Syn are detected throughout the length of the fibrils and similar proportions were found in the aggregated insoluble fraction. (4) Soluble oligomeric species with identical morphological features and molecular mass could be recapitulated with labeled α-Syn. Moreover, size exclusion elution profiles for both labeled and unlabeled α-Syn were also identical (data not shown), indicating that neither form was preferentially misfolded. Such concordance suggests that addition to α-Syn of a fluorescent moiety does not result in significant alterations in its properties in vitro.

Upon assembly into fibrils, labeled α-Syn also exhibited increased ThT fluorescence, confirming the presence of β-sheet rich structure. While high FP values were also associated with the presence of larger, more immobile fibrils, we found that increases in FP preceded that of increased amyloid dye binding. Further investigation revealed that, in addition to mature α-Syn fibrils, the FP method is capable of detecting oligomeric forms of α-Syn.

Compounds that either inhibit or promote fibril formation have been identified using ThT and Congo Red to monitor in vitro fibrillization (*19*, *20*, *36*, *37*). We show here that, similar to amyloid binding dyes, FP positively identified compounds that inhibit α-Syn fibrillization. Unlike ThT or K114, FP can distinguish compounds that prevent nucleation from those that inhibit elongation, including those that generate soluble multimeric intermediates. When combined with a suitable amyloid dye, FP allows the monitoring of the fibrillization process by providing simultaneous readouts of both molecular mass and fibrillar β-sheet content. By employing fluorophores with spectral properties that do not interfere or overlap with ThT, we demonstrate that this strategy can be applied to assess the ability of compounds to inhibit α-Syn fibril formation. By reading the samples at two different wavelengths, anomalous results arising from optical (fluorescence) interference can be more easily detected. The capability to monitor individual samples over extended periods in a real-time and nondestructive manner is particularly useful given the considerable time required for α-Syn fibril assembly relative to other amyloidgenic proteins (e.g., Aβ). The simplicity of this technique has also facilitated our efforts to scale the assay to a 384-well plate format. Together, these properties make FP highly amenable to automation and large scale HTS screening of compound libraries for potential modulators of α-Syn misfolding. Since α-Syn end products generated using this method are labeled, additional analysis by fluorescence microscopy is a potential option.

In summary, despite significant challenges to PD drug discovery, advances in PD research suggest that agents designed to inhibit or reverse the fibrillization and deposition of α-Syn could have potential disease modifying effects. The realization of this drug discovery goal would certainly revolutionize the treatment of PD thereby offering prospects for arresting or reversing the progression of PD as well as preventing the onset of this and related neurodegenerative synucleinopathies.

ACKNOWLEDGMENT

We are indebted to the patients and their caregivers who have facilitated the study of these neurodegenerative diseases. V.M.Y.L. is the John H. Ware 3rd Professor of Alzheimer's Disease Research. J.Q.T. is the William Maul Measey−Truman G. Schnabel, Jr., Professor of Geriatric Medicine and Gerontology. This research was supported by the NIH (P01 AG09215, NS053488) and the Picower Foundation.

REFERENCES

1. Norris, E. H., Giasson, B. I., and Lee, V. M. Y. (2004) *Stem Cells Dev. Dis. 60*, 17−54.
2. Savitt, J. M., Dawson, V. L., and Dawson, T. M. (2006) *J. Clin. Invest. 116*, 1744−1754.
3. Spillantini, M. G., Crowther, R. A., Jakes, R., Hasegawa, M., and Goedert, M. (1998) *Proc. Natl. Acad. Sci. U.S.A. 95*, 6469−6473.
4. Spillantini, M. G., Crowther, R. A., Jakes, R., Cairns, N. J., Lantos, P. L., and Goedert, M. (1998) *Neurosci. Lett. 251*, 205−208.
5. Lee, V. M. Y., and Trojanowski, J. Q. (2006) *Neuron 52*, 33−38.
6. Hashimoto, M., Hsu, L. J., Sisk, A., Xia, Y., Takeda, A., Sundsmo, M., and Masliah, E. (1998) *Brain Res. 799*, 301−306.
7. Wood, S. J., Wypych, J., Steavenson, S., Louis, J. C., Citron, M., and Biere, A. L. (1999) *J. Biol. Chem. 274*, 19509−19512.
8. Volles, M. J., and Lansbury, P. T. (2002) *Biochemistry 41*, 4595−4602.

9. Kayed, R., Head, E., Thompson, J. L., McIntire, T. M., Milton, S. C., Cotman, C. W., and Glabe, C. G. (2003) *Science 300*, 486−489.
10. El, Agnaf, O. M. A., Salem, S. A., Paleologou, K. E., Curran, M. D., Gibson, M. J., Court, J. A., Schlossmacher, M. G., and Allsop, D. (2006) *FASEB J. 20*, 419−425.
11. Polymeropoulos, M. H., Lavedan, C., Leroy, E., Ide, S. E., Dehejia, A., Dutra, A., Pike, B., Root, H., Rubenstein, J., Boyer, R., Stenroos, E. S., Chandrasekharappa, S., Athanassiadou, A., Papapetropoulos, T., Johnson, W. G., Lazzarini, A. M., Duvoisin, R. C., DiIorio, G., Golbe, L. I., and Nussbaum, R. L. (1997) *Science 276*, 2045−2047.
12. Singleton, A. B., Farrer, M., Johnson, J., Singleton, A., Hague, S., Kachergus, J., Hulihan, M., Peuralinna, T., Dutra, A., Nussbaum, R., Lincoln, S., Crawley, A., Hanson, M., Maraganore, D., Adler, C., Cookson, M. R., Muenter, M., Baptista, M., Miller, D., Blancato, J., Hardy, J., and Gwinn-Hardy, K. (2003) *Science 302*, 841.
13. Spillantini, M. G., Schmidt, M. L., Lee, V. M. Y., Trojanowski, J. Q., Jakes, R., and Goedert, M. (1997) *Nature 388*, 839−840.
14. Uversky, V. N., Li, J., and Fink, A. L. (2001) *J. Biol. Chem. 276*, 10737−10744.
15. Bertoncini, C. W., Jung, Y. S., Fernandez, C. O., Hoyer, W., Griesinger, C., Jovin, T. M., and Zweckstetter, M. (2005) *Proc. Natl. Acad. Sci. U.S.A. 102*, 1430−1435.
16. Crystal, A. S., Giasson, B. I., Crowe, A., Kung, M. P., Zhuang, Z. P., Trojanowski, J. Q., and Lee, V. M. Y. (2003) *J. Neurochem. 86*, 1359−1368.
17. Khurana, R., Ionescu-Zanetti, C., Pope, M., Li, J., Nielson, L., Ramirez-Alvarado, M., Regan, L., Fink, A. L., and Carter, S. A. (2003) *Biophys. J. 85*, 1135−1144.
18. Khurana, R., Coleman, C., Ionescu-Zanetti, C., Carter, S. A., Krishna, V., Grover, R. K., Roy, R., and Singh, S. (2005) *J. Struct. Biol. 151*, 229−238.
19. Masuda, M., Suzuki, N., Taniguchi, S., Oikawa, T., Nonaka, T., Iwatsubo, T., Hisanaga, S., Goedert, M., and Hasegawa, M. (2006) *Biochemistry 45*, 6085−6094.
20. Conway, K. A., Rochet, J. C., Bieganski, R. M., and Lansbury, P. T. (2001) *Science 294*, 1346−1349.
21. Glabe, C., Kayed, R., Sokolov, Y., and Hall, J. (2004) *Neurobiol. Aging 25*, S75−S76.
22. Conway, K. A., Lee, S. J., Rochet, J. C., Ding, T. T., Williamson, R. E., and Lansbury, P. T. (2000) *Proc. Natl. Acad. Sci. U.S.A. 97*, 571−576.
23. Emadi, S., Barkhordarian, H., Wang, M. S., Schulz, P., and Sierks, M. R. (2007) *J. Mol. Biol. 368*, 1132−1144.
24. Kaylor, J., Bodner, N., Edridge, S., Yamin, G., Hong, D. P., and Fink, A. L. (2005) *J. Mol. Biol. 353*, 357−372.
25. Giese, A., Bader, B., Bieschke, J., Schaffar, G., Odoy, S., Kahle, P. J., Haass, C., and Kretzschmar, H. (2005) *Biochem. Biophys. Res. Commun. 333*, 1202−1210.
26. Levison, S. A., Dandliker, W. B., Brawn, R. J., and Vanderlaan, W. P. (1976) *Endocrinology 99*, 1129−1143.
27. Giasson, B. I., Uryu, K., Trojanowski, J. Q., and Lee, V. M. Y. (1999) *J. Biol. Chem. 274*, 7619−7622.
28. Rusinova, E., Tretyachenko-Ladokhina, V., Vele, O. E., Senear, D. F., and Ross, J. B. A. (2002) *Anal. Biochem. 308*, 18−25.
29. Giasson, B. I., Murray, I. V. J., Trojanowski, J. Q., and Lee, V. M. Y. (2001) *J. Biol. Chem. 276*, 2380−2386.
30. Giasson, B. I., Duda, J. E., Quinn, S. M., Zhang, B., Trojanowski, J. Q., and Lee, V. M. Y. (2002) *Neuron 34*, 521−533.
31. Brown, M. P., and Royer, C. (1997) *Curr. Opin. Biotechnol. 8*, 45−49.
32. Schmidt, M. L., Schuck, T., Sheridan, S., Kung, M. P., Kung, H., Zhuang, Z. P., Bergeron, C., Lamarche, J. S., Skovronsky, D., Giasson, B. I., Lee, V. M. Y., and Trojanowski, J. Q. (2001) *Am. J. Pathol. 159*, 937−943.
33. Ding, T. T., Lee, S. J., Rochet, J. C., and Lansbury, P. T. (2002) *Biochemistry 41*, 10209−10217.
34. Norris, E. H., and Giasson, B. I. (2005) *Antioxid. Redox Signaling 7*, 673−684.
35. Li, J., Zhu, M., Manning-Bog, A. B., Di, Monte, D. A., and Fink, A. L. (2004) *FASEB J. 18*, 962−964.
36. Zhu, M., Rajamani, S., Kaylor, J., Han, S., Zhou, F. M., and Fink, A. L. (2004) *J. Biol. Chem. 279*, 26846−26857.
37. El Agnaf, O. M. A., Paleologou, K. E., Greer, B., Abogrein, A. M., King, J. E., Salem, S. A., Fullwood, N. J., Benson, F. E., Hewitt, R., Ford, K. J., Martin, F. L., Harriot, P., Cookson, M. R., and Allsop, D. (2004) *FASEB J. 18*, 1315−1317.

BI701128C